Catalysis Today xxx (2016) xxx–xxx

Contents lists available at ScienceDirect

Catalysis Today

journal homepage: www.elsevier.com/locate/cattod

Bimetallic carbon nanocatalysts for methanol steam reforming in conventional and membrane reactors

Aleksandra A. Lytkina[a,*], Natalia V. Orekhova[a], Margarita M. Ermilova[a], Sergey V. Belenov[b], Vladimir E. Guterman[b], Mikhail N. Efimov[a], Andrey B. Yaroslavtsev[a]

[a] A.V. Topchiev Institute of Petrochemical Synthesis, Russian Academy of Sciences, Leninsky Pr. 29, Moscow, Russia
[b] Chemistry Department, Southern Federal University, Zorge St., 7, Rostov-on-Don, Russia

ARTICLE INFO

Article history:
Received 10 September 2015
Received in revised form 1 December 2015
Accepted 14 January 2016
Available online xxx

Keywords:
Hydrogen production
Methanol steam reforming
Carbon
Bimetallic catalyst
Membrane catalytic system

ABSTRACT

In this paper we report the results obtained by a comparative study of catalytic activity of bimetallic (Ru–Rh, Ni–Cu) catalysts synthesized on a surface of different carbon supports: detonation nanodiamonds (DND), infrared pyrolyzed polyacrylonitrile, carbon black Vulcan-XC-72, in steam reforming of methanol (MSR) for hydrogen production. All obtained catalysts were characterized by N_2 physisorption, SEM, TEM, FTIR spectroscopy, X-ray diffraction. It was shown, that activity of catalysts and products distribution depends on metal type, support material and the specific surface area. Support effect was investigated for Ru–Rh system. DND showed the best properties as a catalyst support. Ru–Rh system is more active than Cu–Ni as it is shown on the example of DND supported catalysts. Comparative study between conventional (CR) and membrane (MR) reactors was carried out. MR represented a flow system with a plane Pd-containing membrane. The effect of different catalysts on the MR performances as well as a general comparison of the experimental results was considered. Obtained results demonstrate the ability of the membrane to increase the reaction conversion. The hydrogen stream produced from the MR is ultra pure: especially, it is CO-free and thus suitable to be directly fed to a polymer electrolyte membrane fuel cell.

1. Introduction

Atmosphere of big cities becomes more polluted by products of incomplete combustion, nitrogen and sulfur oxides as a result of technical progress. This significantly affects on ecology. From this viewpoint, an attractive technology is a conversion of chemical energy into electrical one by fuel cells (FC) which produces water only. However, absence of hydrogen in nature in a pure form defines urgency of the problem of its synthesis [1]. Methane can be considered as a promising feedstock for technical hydrogen obtaining. Nevertheless, its nonoxidative coupling is accompanied by significant energy consumption and occurs at high temperatures with low productivity or requires a forced activation [2]. Steam reforming of methane [3,4], or its high-temperature conversion, flowing due to partial oxidation by oxygen, are much more economically feasible [5]. However, process leads to a syngas evolution, wherein the ratio of hydrogen to CO is usually less than 2:1 [6]. Such hydrogen is unsuitable for low-temperature fuel cells due to poisoning of its catalyst even in the presence of trace impurities of CO [7,8].

Steam reforming of alcohols, which are much more chemically active than methane, proceeds at considerable lower temperatures [8–12]. It is important that alcohol, produced from biomass (bio-alcohol), can be considered as a renewable raw material. Methanol has a number of advantages compared with other precursors for hydrogen production. Since it has only one carbon atom, methanol is one of the simplest compounds that dramatically reduces the number of reaction byproducts. The absence of the C—C bonds in the molecule allows to conduct reforming at relatively low temperatures (200–350 °C) [13]. Methanol is a toxic substance, but at the same time it is biodegradable, it is a liquid at ambient conditions.

In the MSR in addition to the target Reaction (1):

$$CH_3OH + H_2O \leftrightarrow CO_2 + 3H_2, \quad \Delta H^\circ_{298K} = 49.7\ kJmol^{-1} \qquad (1)$$

also the reactions of methanol decomposition (2), and water-gas shift (WGS) Reaction (3) occur:

$$CH_3OH \leftrightarrow CO + 2H_2, \Delta H^\circ_{298\ K} = 90.2\ kJmol^{-1} \qquad (2)$$

$$CO + H_2O \leftrightarrow CO_2 + H_2, \quad \Delta H^\circ_{298K} = -41.2\ kJmol^{-1} \qquad (3)$$

* Corresponding author.
E-mail address: lytkina@ips.ac.ru (A.A. Lytkina).

http://dx.doi.org/10.1016/j.cattod.2016.01.003
0920-5861/

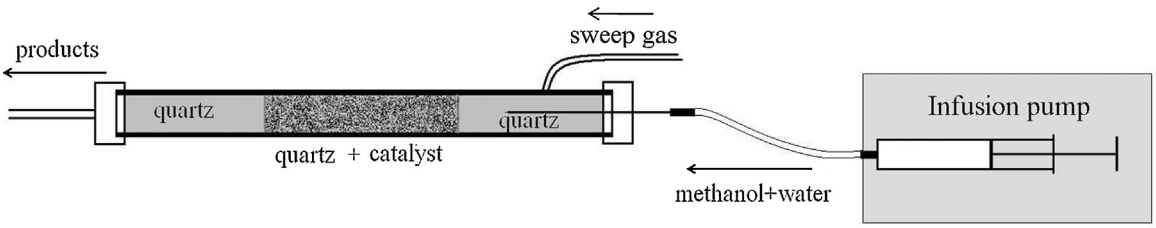

Fig. 1. Scheme of the conventional flow reactor.

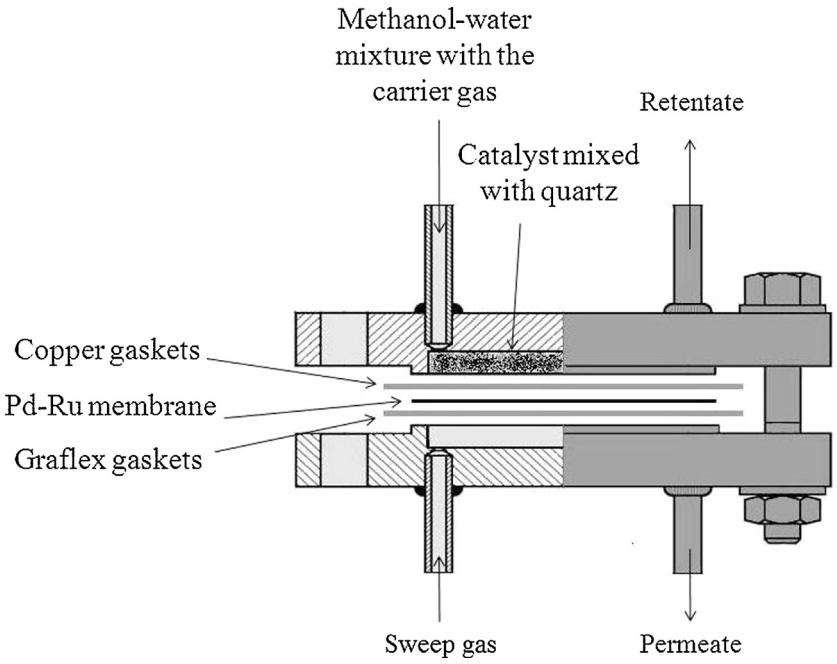

Fig. 2. Scheme of the membrane reactor.

Reactions (1) and (2) require heat supplying, and Reaction (3) occurs with heat evolution.

As a result a mixture of hydrogen and carbon oxides is obtained; the ratio of products depends on the process conditions and the catalyst used.

Carbon monoxide is usually an undesirable product. Its formation according to Reaction (2) reduces hydrogen yield. The problem of reducing the amount of carbon monoxide is very crucial because it poisons the Pt-containing catalysts in a fuel cell. It imposes strict requirements to hydrogen purity and emphasizes the importance of the catalyst choice for MSR reaction [5,7].

Deactivation of catalysts for MSR can occur generally owing to a change in oxidation state, sintering of metal particles or coke deposition. It is known that resistance to deactivation of monometallic catalysts can be improved by adding promoters [14]. Cu-containing composites with various additives that increase the stability of the catalyst and the hydrogen yield are considered as the good catalysts for the MSR. For example, addition of Ni to the copper monometallic catalyst significantly increases its resistance to deactivation [15]. It was also shown that noble metals such as Rh, Ir, Pt, Ru, Pd, have high activity in steam reforming of alcohols [16]. Moreover, Rh is regarded as one of the most active in a number of noble metals [17]. In the works [18–22] Ru is considered as a promising catalyst for alcohol steam reforming processes also. The authors of [23] have reported a significant selectivity improvement of catalysts doped by Rh, owing to its activity in the WGS reaction. However, application of noble metals in catalysis is limited because of their high-value [24]. Therefore, of great interest are catalysts with a low content of noble metals [25], as well as materials containing several metals [26–28].

An important issue is to increase selectivity of the composite and its resistance to carbonization. Therefore, new fine carbon materials are of great interest, such as nanotubes, nanowires, graphene and nanodiamonds (DND). The unique properties of these materials make them appropriate for use as catalyst supports [12,29,30]. It is important that application of carbon carriers mainly eliminates the problem of a catalyst carbonization. Moreover DND or fine-dispersed carbon black have high specific surface area and mainly mesoporous structure.

The problem of high purity hydrogen production (which is needed for PEMFC) can be successfully solved in the case of using of membrane catalysis by selective removal of hydrogen [13,31,32]. During the last few decades a large number of researches were devoted to carrying out of alcohols SR in membrane reactors (MR) [33–37]. The advantage of this approach lies not only in production of impurities free hydrogen, but in an increase of its yield also by selective extraction from reaction zone.

Compared with pure Pd membranes, membranes, made of some Pd alloys, have several advantages because of their higher hydrogen permeability, strength, thermal stability and catalytic activity [38–42]. The introduction of even small amounts (~1 wt%) Ru into palladium increases mechanical stability of the membrane during thermal cycling in hydrogen [43].

The aim of the work was to search new productive and selective to hydrogen catalysts for MSR on various carbon supports (DND, IR pyrolyzed polyacrylonitrile, carbon black Vulcan) and to

Please cite this article in press as: A.A. Lytkina, et al., Bimetallic carbon nanocatalysts for methanol steam reforming in conventional and membrane reactors, Catal. Today (2016), http://dx.doi.org/10.1016/j.cattod.2016.01.003

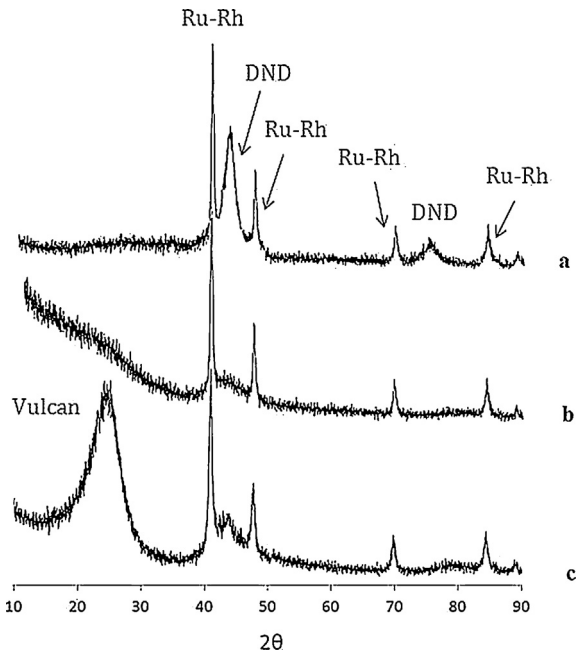

Fig. 3. XRD patterns of the catalysts in the region of $2\theta = 10–90^{\circ}$: (a) Ru–Rh/DND; (b) Ru–Rh/PAN; (c) Ru–Rh/Vulcan.

study of obtained catalysts behavior in the conventional tube and membrane reactors. Comparing of catalytic activity in MSR reaction of Ru–Rh and more cheap Ni-Cu systems, supported on DND was of interest also.

2. Experimental

2.1. Synthesis of the catalysts and technique of the catalytic experiments

Ru–Rh/C catalysts were prepared by reduction of metals precursors (ruthenium(III) chloride and rhodium (III) chloride) at room temperature in a liquid phase using 0.5 M $NaBH_4$ as a reducing agent. As a medium for the synthesis aqueous solution of ethylene glycol (EG 50% by volume) was used. As support detonation nanodiamonds, Vulcan XC-72 and IR pyrolyzed polyacrylonitrile were used. Calculated amount of carbon support was added into the metal-containing precursor solution and dispersed using an ultrasonic homogenizer US Soniprep to obtain a homogeneous suspension. The amount of precursors was calculated based on the total metal content in a material after their complete reduction of 7.5 wt.% and metals atomic ratio of 1:1. The mixture was brought up to pH 10 by an aqueous solution of ammonia, and then during intensive stirring threefold excess of a freshly prepared aqueous solution of 0.5 M $NaBH_4$ was added. The solution was kept for 40 min under constant stirring for complete reduction of both metals. Obtained suspension was filtered using a Buchner funnel, washed repeatedly by deionized water and acetone. A resulting powder was dried at 80 °C for 3 h. Obtained catalysts were treated with H_2 (5%)/Ar (20 ml/min) for 3 h at 350 °C for metal oxides reduction.

For a synthesis of the Ni–Cu/DND catalyst DND powder was sequentially impregnated with aqueous solutions of $Cu(NO_3)_2{\cdot}3H_2O$ (>98%) and $Ni(NO_3)_2{\cdot}6H_2O$ (≥98.5% ALDRICH) at an appropriate concentration calculated so that the total metal content was equal to 20% from the support weight; nickel and copper ratio was 1:4 (previously it has been shown that this ratio is close to optimal for the system Ni–Cu [44]). So-prepared suspension was dispersed in an ultrasonic bath for 1 h, and then excess of water was evaporated at 100 °C in a drying oven. The obtained catalysts were annealed at 400 °C in inert atmosphere for 3 min. Further, they were treated with H_2 (5%)/Ar (20 ml/min) for 3 h at 350 °C. Thus, three bimetallic Ru–Rh/C samples were prepared, differing in nature of the support and the catalyst Ni–Cu/DND.

Steam reforming of methanol was carried out at atmospheric pressure in the conventional stainless steel tubular reactor (Fig. 1) in a temperature range of 200–400 °C. The tube length was of 21.5 cm and inner diameter was of 0.9 cm. A catalyst sample (loading was 0.3 g) was mixed with granular silica and placed to the middle of the reactor tube. Heating of the reactor up to a work temperature was carried out by electric furnace during constant argon flow (20 cm^3/min); the temperature of the reactor was measured by a chromel–alumel thermocouple. Catalysts were reduced in situ with a mixture of H_2 (5%)/Ar (20 cm^3/min) at a temperature of 350° C for 3 h before every experiment. During the reaction, argon flow rate was constant and equaled to 20 cm^3/min. A liquid mixture of methanol and water, with a stoichiometric molar ratio of 1:1 was fed to an evaporator using an infusion pump Instilar 1488 Dixion. Unreacted alcohol and water were condensed in a glass collector, cooled to +1° C. Analysis of uncondensed reaction products was performed by gas chromatograph LHM 8MD with a thermal conductivity detector, helium as a carrier gas and columns with stationary phases Porapak T for water, methanol and other oxygenates and activated carbon for CO and CO_2. Concentrations of hydrogen and methane in products were measured by a chromatograph Chrom-4 with a thermal conductivity detector and a CaA Zeosorb column, with Ar as a carrier gas. Chromatograms were processed using software package Ecochrom (Fig. 1).

The second series of MSR experiments was carried out in the MR. The samples of catalysts mixed with granulated quartz (fraction 1–3 mm) were placed into the reaction zone of the MR, which scheme is shown on a Fig. 2. The reactor consisted of two stainless steel cylindrical-shaped compartments, divided by a pinhole-free foil membrane of Pd–Ru alloy (6 mass% Ru). The thicknesses of investigated membranes were 12 and 70 microns. Two gaskets made of copper and of Graflex, ensured a hermeticity of the reactor. Experiments in MR were carried out at the temperatures of 200–350 °C. The flow rate of sweep gas on a permeate and reten-

Please cite this article in press as: A.A. Lytkina, et al., Bimetallic carbon nanocatalysts for methanol steam reforming in conventional and membrane reactors, Catal. Today (2016), http://dx.doi.org/10.1016/j.cattod.2016.01.003

tate side was of 20 cm^3/min. The reaction products were analyzed by the method described above.

The alcohol conversion degree, X (%) was calculated from the results of analysis by using the following equation:

$$X = \frac{[\varphi_0 - \varphi_1]}{\varphi_0} \times 100$$

where φ_0 and φ_1 are the initial and the final ethanol concentration respectively.

The yields of products was assessed as the amount of the corresponding reaction product (in moles) forming per gram of metal in the catalyst per hour.

2.2. Structure and morphology of the catalysts

The specific surface area and pore size were determined using the N_2 adsorption BET method with an ASAP-2020N (Micromeritics Co., USA) instrument. X-ray diffraction analysis (XRD) of the samples was performed on X-ray diffractometer Rigaku D/Max-2200, CuKα1—radiation. For spectra processing and qualitative analysis Rigaku Application Data Processing software package was used. Particles sizes (coherent scattering region) were estimated from the width of the XRD patterns peaks by Scherrer equation:

$$d = \frac{k \times \lambda}{(B - b) \times \cos\theta} \quad (4)$$

where $k = 0.89$—Scherrer constant; $\lambda = 1.5406$ Å—the wave length of used radiation; B—a width at half maximum(2θ); b—instrumental broadening (2θ); θ—the angle of a peak position.

TEM images were taken with a Transmission Electron Microscope JEM 2100 with an acceleration voltage of 200 kV, with a point resolution 0.23 nm. The chemical analysis data and SEM images were obtained using the Scanning Electron Microscopy technique on Carl Zeiss NVision 40 with adapter for element analysis; an acceleration voltage was 200 kV.

IR spectra of the supports in the form of pellets with Ge were recorded before using in MSR process by using the FTIR spectrometer IFS-66-v/s in the wavelength range 600–4000 cm^{-1}.

3. Results and discussion

3.1. Structural and morphological characterization of the catalysts

Under the study we have investigated three types of carbon supports differing in surface area and nature of functional groups on the surface:

1) *Detonation nanodiamond*, which is a product of detonation synthesis. DND nanoparticles consist of a core, having diamond lattice (carbon atoms in sp3-hybridisation), and amorphous carbon shell with a thickness up to four carbon atoms. Furthermore, DND surface contains a large amount of oxygen-containing functional groups that provide good adsorption properties of the material [45].
2) *IR pyrolyzed polyacrylonitrile*, this material was prepared by IR annealing of polyacrylonitrile (PAN) at the temperature of about 800 °C, and its subsequent activation by potassium hydroxide. IR PAN is a microporous material with a high surface area and it contains carbon with different hybridization and structure.
3) *Carbon Black Vulcan* is a commercial product obtained by pyrolysis of gaseous hydrocarbons. Vulcan contains globular amorphous carbon with a basic particle size of about 30 nm.

Fig. 3 shows X-ray patterns of catalysts supported on different types of carbon materials. On roentgenograms broad peaks with maxima at 43.6° corresponding to nanodiamonds (Fig. 3a) and amorphous halo of IR PAN (Fig. 3b) are seen. It can be noted that carbon black Vulcan has some order in its structure, manifested in broad reflections with peaks at 25, 43 and 78.5° (Fig. 3c). Narrower peaks correspond to alloy Ru–Rh, reflexes maximums of this alloy are located between the positions which are characteristic for the individual metals. The unit cell parameters for the resulting alloys are equal to 0.38044 ± 0.0002 nm (Fig. 4).

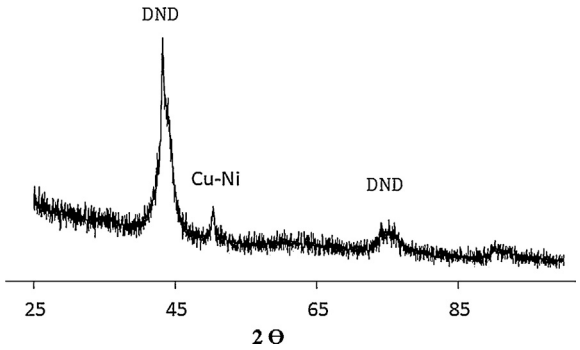

Fig. 4. XRD patterns of the catalyst: Ni–Cu/DND.

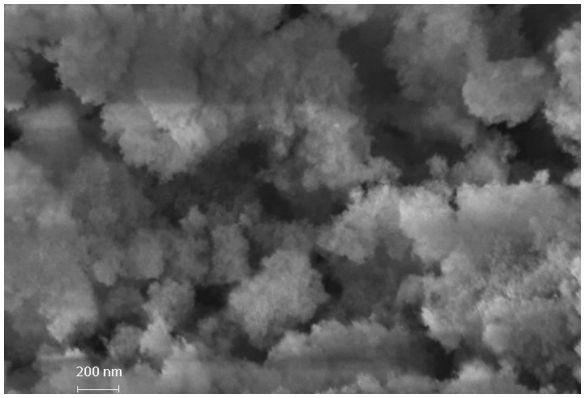

Fig. 5. SEM image of the catalyst: Ru–Rh/DND.

The XRD pattern of the catalyst Ni–Cu/DND are similar to described above (Fig. 4). It is possible also to identify the broad lines of nanodiamond and peaks of Ni–Cu alloy with unit cell parameter of 0.3616 ± 0.0009 nm.

Table 1 shows the specific surface area of the supports, the composites, micropore area, and the average particle sizes of composites estimated by the BET method and average metal particle sizes, estimated from the width of the XRD (coherent scattering region (CSR)). Obviously, the specific surface area is determined by dispersion degree of a carbon support. Thus, the specific surface area decreases in a line of PAN » DND> Vulcan. Average particle sizes, estimated by BET technique, correspond mainly to average sizes of carbon particles. This follows from its higher content. At the same time, sizes of metal particles are similar in all cases, according to the XRD reflexes widths. It should be noted also that significantly larger specific surface area of PAN, according to BET data, primarily determined by its porosity.

According to the SEM data, all samples represent tracery agglomerates with a size of 50–300 nm, consisting of substantially smaller particles (Fig. 5). From the data obtained by microprobe analysis, the ratio of ruthenium and rhodium in composites corresponds to 1.5:1, which is slightly higher than the initial load. The ratio of nickel and copper in the sample Ni–Cu/DND corresponds to initial load of 1:4.

Please cite this article in press as: A.A. Lytkina, et al., Bimetallic carbon nanocatalysts for methanol steam reforming in conventional and membrane reactors, Catal. Today (2016), http://dx.doi.org/10.1016/j.cattod.2016.01.003

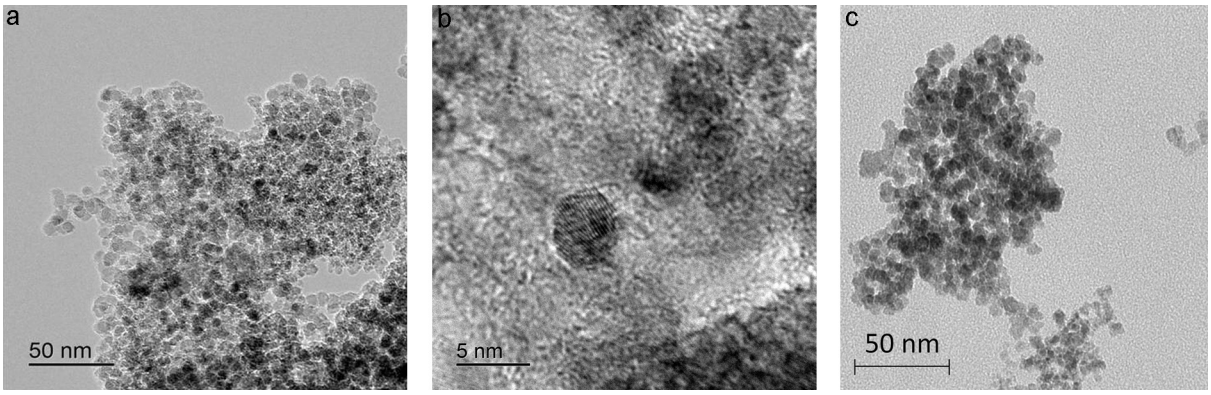

Fig. 6. TEM images of the Ru–Rh/DND (a, b) and Ni–Cu/DND (c) catalysts.

Table 1
The specific surface area and average nanoparticle sizes of obtained materials.

Support		Catalyst			Average particle size (nm)	
	BET surface area (m^2/g)		BET surfacearea (m^2/g)	Micropore area (m^2/g)	BET	CSR (metals)
DND	286 ± 3	Ru–Rh/DND	289 ± 3	15 ± 3	20	13 ± 1
		Ni–Cu/DND	230 ± 3	14 ± 3	25	12 ± 1
Vulcan	200 ± 3	Ru–Rh/Vulcan	206 ± 3	67 ± 3	30	13 ± 1
PAN	1880 ± 3	Ru–Rh/PAN	1600 ± 3	1124 ± 3	4	13 ± 1

TEM data provide more information about the obtained samples. They evidence that the average particles size of metals is of 5–15 nm in all studied composites (Fig. 6). Note that this size is somewhat smaller than value, estimated from the X-ray peaks width, which probably is a result of a higher reflections intensity of roentgenograms from the larger particles. Similar patterns are discussed in detail in [46]. At the same time the atomic layers of Ru–Rh alloy with interplanar distances, corresponding to XRD reflexes, are good seen on separate micrographs.

3.2. Activity of the catalysts in steam reforming of methanol

3.2.1. Conventional reactor

According to the obtained data, the achieved methanol conversion was not lower than 85% for all catalysts at temperatures of about 300 °C. With further temperature increase the process becomes less selective toward to the hydrogen production. Fig. 7 shows the temperature dependences of hydrogen and carbon monoxide flows on the Ru–Rh/DND and Cu–Ni/DND catalysts.

It is easy to see that the catalyst based on Ru–Rh alloy differs with significantly higher activity as compared with Cu–Ni. At the same time, it should be noted that at low temperatures Cu–Ni/DND catalyst is more selective. Equivalent flow of CO on Cu–Ni catalyst is achieved at temperatures of about 60° higher than on Ru–Rh. At temperatures lower than 270 °C mostly the Reaction (1) proceeds on Cu–Ni catalyst, and produced hydrogen is substantially free of CO.

At the same time, nature of the support plays an important role in MSR mechanism. Fig. 8 shows plots of hydrogen flow rate of the temperature on supported catalysts Ru–Rh/DND, Ru–Rh/Vulcan and Ru–Rh/PAN. Among the composites the highest catalytic activity was shown by the catalyst Ru–Rh/DND. Herewith activity of the catalysts decreased in the line of DND> PAN> Vulcan. At the same time, the catalyst supported on carbon black Vulcan was the most selective toward the process, proceeding according to the Reaction (1).

Maximum amount of hydrogen at 300–310 °C was obtained on the DND supported catalyst, which is 2.3 moles from 3 theoretically possible. The similar amount of hydrogen can be obtained on the catalyst Ru–Rh/PAN only at 350 °C, but in this case, the amount of emitted CO is 30% higher than in the case of DND.

Obtained results indicate a significant influence of a support nature on the rate and selectivity of steam reforming of methanol. The lowest activity of the catalysts based on carbon black Vulcan could be explained by less developed surface area. However the highest activity of the catalysts supported on nanodiamonds, compared with PAN contradicts this assertion. In this case, the specific surface area of nanodiamonds approximately 6.5 times lower. It could be assumed that nanodiamonds have their own catalytic activity in MSR reaction. Indeed, we have previously observed a similar property of DND in the process of steam reforming of ethanol [12]. Own catalytic activity is observed for them, in case of MSR too (see. Fig. 8a). However, its magnitude is more than two orders lower than one obtained on Ru–Rh containing catalysts at equivalent temperatures.

The obtained data leads to the conclusion that both a metal and the carrier involved in the catalytic process. FTIR spectra of PAN and Vulcan (Fig. 9, curves 2 and 3) are nearly identical and correspond to highly oxidized carbon with a high content of C—O—C bonds, most likely in cyclic unsaturated compounds with a low content of conjugated bonds on the surface (1580, 1485 cm^{-1}). There is a small amount of saturated CH bonds (2800–2980 cm^{-1}) as well as carbonyl groups (1730–1710 cm^{-1}), but their content is negligible. The hydroxyl groups on the surface of Vulcan and PAN are practically absent —there are no bands in the region of 3400 and 1630 cm^{-1}.

The surface of nanodiamonds contains a large amount of hydroxyl groups. Position of C—O bonds in the spectrum is shifted to shorter wavelengths (950 cm^{-1}). This evidences that C—O bonds on the DND surface are part of the functional groups —COOH, COOR. Ether bonds are present also because the spectrum of DND exhibits disintegration of the band. These surface species can actively adsorb water molecules by formation of hydrogen bonds like H—O—H···O. In turn, methanol molecules are adsorbed on the metal surface (Fig. 10). Then an activated oxygen of water heads to a carbon atom of methanol and results in carbon dioxide molecules formation. Obviously, this process can only takes place at the metal-carrier boundary, the development of which is determined only by the

Please cite this article in press as: A.A. Lytkina, et al., Bimetallic carbon nanocatalysts for methanol steam reforming in conventional and membrane reactors, Catal. Today (2016), http://dx.doi.org/10.1016/j.cattod.2016.01.003

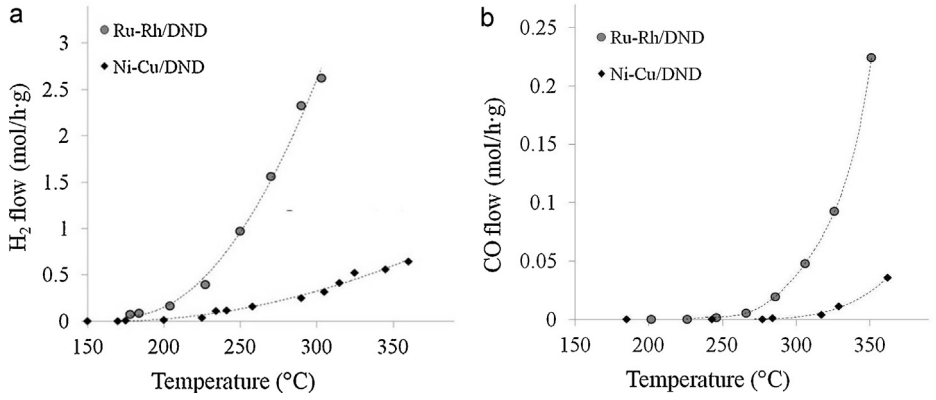

Fig. 7. Temperature dependence of (a) H_2; (b) CO yields in MSR on the Ru–Rh/DND and Ni–Cu/DND catalysts.

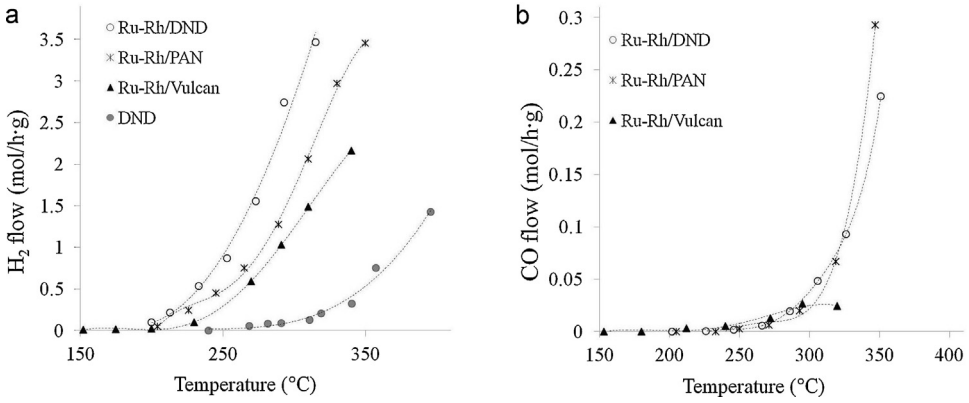

Fig. 8. Temperature dependence of (a) H_2; (b) CO yields in MSR on the obtained catalysts.

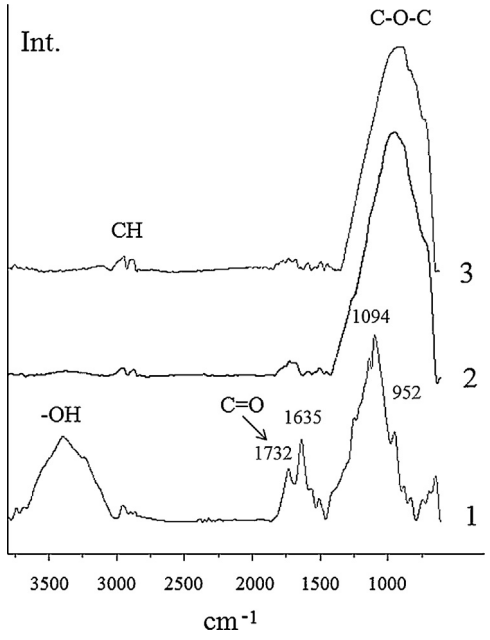

Fig. 9. IR-spectra of DND (1), PAN (2) and Vulcan (3).

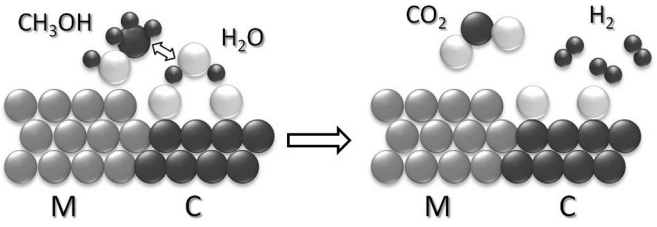

Fig. 10. Scheme of methanol steam reforming process over catalysts surface.

amount of a supported metal and its particle size, and in the first approximation should not depend on support surface area. Another important factor is a concentration of oxygen-containing groups on the surface of the carbon support. All this together determines a higher activity of Ru–Rh catalyst supported on nanodiamonds. During the temperature rise the probability of proceed of Reactions (2) and (3) in the opposite direction increases due to the thermodynamic factors.

The reason for the higher activity of Ru–Rh catalyst in MSR compared to Ni–Cu, probably is a stronger adsorption of methanol. This leads to easier destruction of methanol molecule. On the other hand, it is also leads to an even higher rate of methanol decomposition by Reaction (2) with the release of CO. Nevertheless authors [47] explained it by the fact that on copper surface single-center methanol adsorption via an oxygen atom is preferably, while on the surface of metals of 8–10 groups two-center adsorption also takes place via the of oxygen and carbon atoms. However, this approach, in our opinion, does not explain the significant dependence of catalytic activity on a support nature.

3.2.2. *Membrane reactor*

One of the most promising approaches is to carry out catalytic processes directly in a MR [35,36]. In this case, the use of palladium-containing membranes allows to obtain high-pure hydrogen directly in a catalytic reactor. The examples of such membrane catalytic systems for ESR were recently reported for metal

Please cite this article in press as: A.A. Lytkina, et al., Bimetallic carbon nanocatalysts for methanol steam reforming in conventional and membrane reactors, Catal. Today (2016), http://dx.doi.org/10.1016/j.cattod.2016.01.003

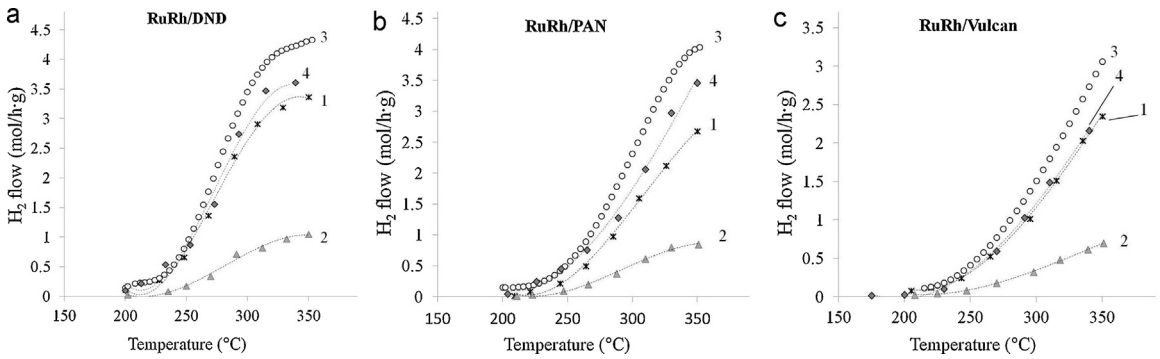

Fig. 11. The flow rates of H_2 in a retentate (curve 1) and permeate zones (curve 2), the total hydrogen flow (curve 3) in the membrane reactor, and in the conventional reactor (curve 4) on the catalysts (a) Ru–Rh/DND; (b) Ru–Rh/PAN; (c) Rh–Ru/Vulcan.

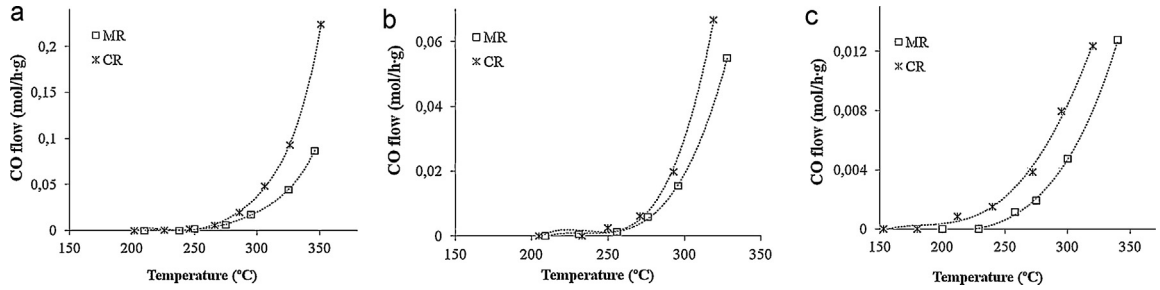

Fig. 12. The flow rates of CO in the membrane and conventional reactors on the catalysts (a) Ru–Rh/DND; (b) Ru–Rh/PAN; (c) Rh–Ru/Vulcan.

catalysts on different supports [36] and for catalytic nanocomposites [33].

Fig. 11 shows the dependence of hydrogen flow rate, obtained in the MR, on temperature with use of the DND, Vulcan and PAN supported catalysts. The total hydrogen yield on all investigated catalysts at high temperatures was approximately 20% higher than in a CR.

Selective hydrogen recovery from the reaction zone shifts the position of equilibrium to the products side and improves conversion of methanol. According to the Reaction (1) it is released 1.5 times more hydrogen on one mole of converted methanol than according to the Reaction (2). This increases hydrogen yield and rise of CO_2 to CO ratio in the reaction products. For example in the case of DND-based catalyst the amount of released CO was close to 5% at ~330 °C in the conventional reformer. At the same time in the MR this value decreased to 1.5%, indicating the selectivity promotion. Decrease of CO quantity in the MR takes place in the case of all catalysts (Fig. 12a–c).

The maximum hydrogen recovery degree for the membrane with a thickness of 70 microns on the Ru–Rh/DND catalyst reached 15% only. It could be expected that the process efficiency will increase significantly when a membrane with thickness of 12 microns will be used. However, hydrogen permeation through this membrane was not reversely proportional to the membrane thickness and increased no more than twice. When the membrane having a thickness of 12 microns was used the maximum degree of hydrogen recovery reached only 25%. Moreover this value was slightly varied in the investigated temperature range.

The mechanism of hydrogen permeation through the Pd-containing membrane includes dissociative adsorption of its molecules and recombination desorption of hydrogen atoms on the entrance and exit surfaces of the membrane, respectively, and diffusion through the membrane body. For relatively thick foil diffusion in the membrane bulk is the rate-limiting step. Therefore, the flow of hydrogen is reversely proportional to the thickness of the membrane and proportional to the difference between the square roots of hydrogen partial pressures in the retentate and permeate zones. Such dependence is called Sieverts law. In the case of thin membranes hydrogen permeation through the membrane is accelerated and its speed is mostly limited by adsorption processes [48]. At the same time, force of Siverts law stopped and the effective value of hydrogen permeability through the membrane decreases. The reasons for deviations from Sieverts law may be poisoning the surface with CO, and the surface processes such as “concentration polarization” [49,50]. This phenomenon is concluded in difficulty of adsorption of permeable species (in this case H_2) due to the presence of some less permeable or non-permeable substances, thus reducing the overall efficiency of the process. In the case of thin foils this effect, called a concentration polarization can be quite substantial. This, unfortunately, decreases the efficiency of the membrane catalysis. It is worth to highlight, that hydrogen, obtained in the permeate side was ultrapure in all cases.

4. Conclusions

Ni–Cu/DND, Ru–Rh/DND, Ru–Rh/PAN, Ru–Rh/Vulcan catalysts for the process of methanol steam reforming were synthesized. Achieved methanol conversion was not lower than 85% for all catalysts at temperatures of about 330 °C. Catalyst based on Ru–Rh alloy differs with significantly higher activity as compared with Ni–Cu. At the same time, at low temperatures Ni–Cu/DND catalyst is more selective.

Although a pure carrier is inactive in MSR, its nature has a significant effect on the activity of the catalytic system. Activity of the catalysts decreased in the line of DND > PAN > Vulcan. At the same time, carbon black Vulcan supported catalyst was the most selective toward to hydrogen production. Maximum amount of hydrogen at 300–310 °C was obtained on the DND supported catalyst, which is 2.3 moles from 3 theoretically possible. Surface of nanodiamonds is rich with oxygen-containing groups, namely —OH, —C=O, —COOH, —COOR. Perhaps the presence of these species determines a higher

Please cite this article in press as: A.A. Lytkina, et al., Bimetallic carbon nanocatalysts for methanol steam reforming in conventional and membrane reactors, Catal. Today (2016), http://dx.doi.org/10.1016/j.cattod.2016.01.003

activity of the supported catalyst DND/Ru–Rh. Their concentration is negligible in the case of PAN and carbon black Vulcan.

Two Pd–Ru membranes with thickness of 70 and 12 microns were investigated in the MR. The maximum hydrogen recovery degree for the membrane with a thickness of 70 microns on the Ru–Rh/DND catalyst reached 15% only. When the membrane having a thickness of 12 microns was used the degree of hydrogen recovery increased to 25%. Comparison of hydrogen permeation through thick and thin membranes showed that in the last case there are deviations from Siverts law. The reasons for deviations from Sieverts law may be poisoning the surface with CO, and the processes proceeding above the membrane surface such as "concentration polarization" which decreases the efficiency of the membrane catalysis.

In spite of this phenomenon in the MR with 12 micron membrane the total hydrogen yield on all investigated catalysts at high temperatures was approximately 20% higher than in the CR. Selective hydrogen recovery from the reaction zone shifts the reaction direction toward the product side and improves methanol conversion and process selectivity.

Acknowledgments

The authors are grateful to Natalia Tabachkova (the Center for Collective Use of Moscow Institute of Steel and Alloys) for the TEM investigation of the samples and Galina Bondarenko for the FTIR experiments.

References

[1] J. Nowotny, T.N. Veziroglu, Int. J. Hydrogen Energy 36 (2011) 13218–13224.
[2] N.L. Basov, M.M. Ermilova, N.V. Orekhova, I.A. Oreshkin, A.B. Yaroslavtsev, Mendeleev Commun. 23 (2013) 69–70.
[3] A. Heinzel, B. Vogel, P. Hiugner, J. Power Sources 105 (2002) 202–207.
[4] Y. Shirasaki, T. Tsuneki, Y. Ota, I. Yasuda, S. Tachibana, H. Nakajima, K. Kobayashi, J. Hydrogen Energy 34 (2009) 4482–4487.
[5] M.V. Tsodikov, A.V. Chistyakov, F.A. Yandieva, V.V. Zmakin, A.E. Gekhman, I.I. Moiseev, CAT Ind. 3 (2011) 4–10.
[6] A.A. Markov, M.V. Patrakeev, I.A. Leonidov, V.L. Kozhevnikov, J. Solid State Electrochem. 15 (2011) 253–287.
[7] K. Ota, Y. Nakagawa, M. Takahashi, J. Electroanal. Chem. 179 (1984) 179–186.
[8] A.B. Yaroslavtsev, A.Yu. Dobrovolsky, N.S. Shaglaeva, L.A. Frolova, E.V. Gerasimova, E.A. Sanginov, Russ. Chem. Rev. 81 (2012) 191–220.
[9] G. Ellert, M.V. Tsodikov, S.A. Nikolaev, V.M. Novotortsev, Russ. Chem. Rev. 83 (2014) 718–732.
[10] L.L. Macarshin, V.N. Parmon, Ros. Khim. J. 50 (2006) 19–25 (in Russian).
[11] N.L. Basov, M.M. Ermilova, N.V. Orekhova, A.B. Yaroslavtsev, Russ. Chem. Rev. 82 (2013) 352–368.
[12] E.Yu. Mironova, M.M. Ermilova, N.V. Orekhova, D.N. Muraviev, A.B. Yaroslavtsev, Catal. Today 236 (2014) 64–69.
[13] A. Iulianelli, P. Ribeirinha, A. Mendes, A. Basile, Renewable and Sustainable Energy Rev. 24 (2014) 355–368.
[14] S. Sá, H. Silva, L. Brandão, J.M. Sousa, A. Mendes, Appl. Catal. B: Environ. 99 (2010) 43–57.
[15] R. Pérez-Hernández, G. Mondragón-Galicia, D. Mendoza-Anaya, J. Palacios, C. Angeles-Chavez, J. Arenas-Alatorre, Int. J. Hydrogen Energy 33 (2008) 4569–4576.
[16] D.R. Palo, A.D. Dagle, J.D. Holladay, Chem. Rev. 107 (2007) 3992–4021.
[17] M. Krumpelt, T. Krause, J. Carter, J. Kopasz, S. Ahmed, Catal Today 77 (2002) 3–16.
[18] A. Iulianelli, T. Longo, S. Liguori, P.K. Seelam, R.L. Keiski, A. Basile, Int. J. Hydrogen Energy 34 (2009) 8558–8565.
[19] M.A. Soria, C. Mateos-Pedrero, A. Guerrero-Ruiz, I. Rodrı×guez-Ramos, Int. J. Hydrogen Energy 36 (2011) 15212–15220.
[20] C.C. Hung, S.L. Chen, Y.K. Liao, C.H. Chen, J.H. Wang, Int. J. Hydrogen Energy 37 (2012) 4955–4966.
[21] I.A. Carbajal Ramos, T. Montini, B. Lorenzut, H. Troiani, F.C. Gennari, M. Graziani, P. Fornasiero, Catal. Today 180 (2012) 96–104.
[22] U. Amjad, A. Vita, C. Galletti, L. Pino, S. Specchia, Ind. Eng. Chem. Res. 52 (2013) 15428–15436.
[23] T. Mondal, K.K. Pant, A.K. Dalai, Appl. Catal. A: Gen. 499 (2015) 19–31.
[24] N. Srisiriwat, S. Therdthianwong, A. Therdthianwong, Int. J. Hydrogen Energy 34 (2009) 2224–2234.
[25] H. Idriss, Ethanol reactions over surfaces of noble metal/cerium oxide catalysts, Platin. Metals Rev. 48 (2004) 105–115.
[26] S. Cavallaro, V. Chiodo, A. Vita, S. Freni, J. Power Sources 123 (2003) 10–16.
[27] E. Vesseli, G. Comelli, R. Rosei, S. Freni, F. Frusteri, S. Cavallaro, Appl. Catal. A: Gen. 281 (2005) 139–147.
[28] J.L. Bi, Y.Y. Hong, C.C. Lee, C.T. Yeh, C.B. Wang, Catal. Today 129 (2007) 322–329.
[29] N.N. Vershinin, O.N. Efimov, V.A. Bakaev, A.E. Aleksenskii, M.V. Baidakova, A.A. Sitnikova, A.Ya. Vul', Fullerenes, Nanotubes and Carbon Nanostructures, 19, 2011, pp. 63–68.
[30] X. Sun, R. Wang, D. Su, Chin. J. Catal. 34 (2013) 508–523.
[31] A. Iulianelli, A. Basile, Catal. Sci. Technol. 1 (2011) 366–379.
[32] E.Yu. Mironova, A.A. Lytkina, M.M. Ermilova, M.N. Efimov, L.M. Zemtsov, N.V. Orekhova, G.P. Karpacheva, G.N. Bondarenko, D.N. Muraviev, A.B. Yaroslavtsev, Int J. Hydrogen Energy 40 (2015) 3557–3565.
[33] B. Krishna, R. Nair, M.P. Harold, Chem. Eng. Sci. 61 (2006) 6616–6636.
[34] A. Basile, A. Parmaliana, S. Tosti, A. Iulianelli, F. Gallucci, C. Espro, J. Spooronen, Catal. Today 137 (2008) 17––22.
[35] A. Iulianelli, S. Liguuori, T. Longo, P. Pinacci, A. Basile, Int J. Hydrogen Energy 35 (2010) 3170–3177.
[36] A. Iulianelli, A. Basile, Int J. Hydrogen Energy 35 (2010) 3159–3164.
[37] P.K. Seelam, S. Liguori, A. Iulianelli, P. Pinacci, V. Calabrò, M. Huuhtanen, R. Keiski, V. Piemonte, S. Tosti, M. De Falco, A. Basile, Catal. Today 219 (2012) 42–48.
[38] F.A. Lewis, Platin. Metals Rev. 26 (1982) 121–128.
[39] N.A. Al-Mufachi, N.V. Rees, R. Steinberger-Wilkens, Renewable Sustainable Energy Rev. 47 (2015) 540–551.
[40] H.W. Abu El Hawa, S.N. Paglieri, C.C. Morris, A. Harale, J.D. Way, J. Membr. Sci. 466 (2014) 151––160.
[41] M.M. Gryaznov, N.V. Ermilova, G.F. Orekhova, Reactors with metal and metal-containing membranes, in: A. Cybulski, J.A. Moulijn (Eds.), Structured Catalysts and Reactors, 2nd ed., Taylor&Francis, London, NY, 2005, p. 579p, Ch. 17.
[42] M. Itoh, M. Saito, C. Yu Li, J. Iwamoto, K. Machida, Chem. Lett. 34 (8) (2005) 1104–1105.
[43] V.M. Gryaznov, A.P. Mishenko, V.P. Poliakova, E.M. Savitskiy, V.S. Smirnov, E.V. Khrapova, Dokl. Akad. Nauk. 211 (1973) 624–628.
[44] A.A. Lytkina, N.A. Zhilyaeva, M.M. Ermilova, N.V. Orekhova, A.B. Yaroslavtsev, Int. J. Hydrogen Energy 40 (2015) 9677–9684.
[45] I.I. Kulakova, Phys. Solid State 46 (2004) 636–643.
[46] S.A. Novikova, G. Yu.Yurkov, A.B. Yaroslavtsev, Mendeleev Commun. 20 (2010) 89–91.
[47] N. Takezawa, N. Iwasa, Catal. Today 36 (1997) 45–56.
[48] L.T. Ward, T. Dao, J. Membr. Sci. 153 (1999) 211–223.
[49] A. Caravella, G. Barbieri, E. Drioli, Sep. Purif. Technol. 66 (2009) 613–624.
[50] W.-H. Chen, M.-H. Hsia, Y.-H. Chi, Y.-L. Lin, C.-C. Yang, Appl. Energy 113 (2014) 41–50.

Please cite this article in press as: A.A. Lytkina, et al., Bimetallic carbon nanocatalysts for methanol steam reforming in conventional and membrane reactors, Catal. Today (2016), http://dx.doi.org/10.1016/j.cattod.2016.01.003